Lipogenesis and redox balance in nitrogen-fixing pea bacteroids

Jason J. Terpolilli[a,b], Shyam, K. Masakapalli[c], Ramakrishnan Karunakaran[b], Isabel Webb[b,c], Rob Green[b], Nicholas J. Watmough[d], Nicholas J. Kruger[c], R. George Ratcliffe[c], Philip S. Poole[b,c,d#]

Centre for Rhizobium Studies, Murdoch University, Perth, Australia[a]; Department of Molecular Microbiology, John Innes Centre, Norwich, United Kingdom[b]; Department of Plant Sciences, University of Oxford, United Kingdom[c]; Centre for Molecular Structure and Biochemistry, University of East Anglia, United Kingdom[d]; Sir Walter Murdoch Adjunct Professor, Murdoch University, Perth, Australia[e]

Running Head: Lipogenesis and redox in N_2-fixing pea bacteroids

[#]Address correspondence to Philip S. Poole, philip.poole@plants.ox.ac.uk

Abstract

Within legume root nodules, rhizobia differentiate into bacteroids that oxidise host-derived dicarboxylic acids, which is assumed to occur via the TCA-cycle to generate NAD(P)H for reduction of N_2. Metabolic flux analysis of laboratory grown *Rhizobium leguminosarum* showed that the flux from ^{13}C-succinate was consistent with respiration of an obligate aerobe growing on a TCA-cycle intermediate as the sole carbon source. However, the instability of fragile pea bacteroids prevented their steady state labelling under N_2-fixing conditons. Therefore, comparitive metabolomic profiling was used to compare free-living *R. leguminosarum* with pea bacteroids. While the TCA-cycle was shown to be essential for maximal rates of N_2-fixation, pyruvate (5.5-fold down), acetyl-CoA (50-fold down), free coenzyme A (33-fold) and citrate (4.5-fold down) were much lower in bacteroids. Instead of completely oxidising acetyl-CoA, pea bacteroids channel it into both lipid and the lipid-like polymer poly-β-hydroxybutyrate (PHB), the latter via a type II PHB synthase that is only active in bacteroids. Lipogenesis may be a fundamental requirement of the redox poise of electron donation to N_2 in all legume nodules. Direct reduction by NAD(P)H of the likely electron donors for nitrogenase, such as ferredoxin, is inconsistent with their redox potentials. Instead, bacteroids must balance the production of NAD(P)H from oxidation of acetyl-CoA in the TCA-cycle with its storage in PHB and lipids.

Importance

Biological nitrogen fixation by symbiotic bacteria (rhizobia) in legume root nodules is an energy-expensive process. Within legume root nodules, rhizobia differentiate into bacteroids that oxidise host-derived dicarboxylic acids, which is assumed to occur via the TCA-cycle to generate NAD(P)H for reduction of N_2. However, direct reduction of the likely

electron donors for nitrogenase, such as ferredoxin, is inconsistent with their redox potentials. Instead bacteroids must balance oxidation of plant-derived dicarboxylates in the TCA-cycle with lipid synthesis. Pea bacteroids channel acetyl-CoA into both lipid and the lipid-like polymer poly-β-hydroxybutyrate, the latter via a type II PHB synthase. Lipogenesis is likely to be a fundamental requirement of the redox poise of electron donation to N_2 in all legume nodules.

Introduction

Biological reduction (or fixation) of atmospheric nitrogen (N_2) to ammonia (NH_3) provides up to 50% of the biosphere's available nitrogen, mostly through symbioses between soil bacteria (rhizobia) and legumes (1, 2). These symbioses are initiated by rhizobia infecting legume roots, resulting in the formation of nodules. Rhizobia differentiate into N_2-fixing bacteroids that express nitrogenase to reduce N_2 to NH_3 under microaerobic conditions (3). Bacteroids receive carbon from the legume while secreting NH_3 to the plant. The overall stoichiometry of N_2 fixation under ideal conditions is:

$$N_2 + 8e^- + 8H^+ + 16ATP \longrightarrow 2NH_3 + H_2 + 16ADP + 16P_i \qquad (1)$$

Thus, eight moles of electrons and protons and 16 moles of ATP reduce a single mole of N_2, making N_2 fixation energetically expensive.

Legumes energise bacteroid N_2 fixation by supplying dicarboxylates, principally malate (4), which must be oxidised to yield ATP and electrons to reduce N_2. Bacteroids metabolise malate by NAD^+-dependent malic enzyme (5-7) and pyruvate dehydrogenase to provide acetyl-CoA, which can be completely oxidised in the TCA-cycle, yielding $FADH_2$ and NAD(P)H. The standard model is that NAD(P)H supplies electrons both to nitrogenase via ferredoxin, or an equivalent low potential electron donor, and to an electron transport chain for ATP synthesis (8, 9).

This is supported by work in *Rhizobium leguminosarum* and *Sinorhizobium meliloti*, where TCA-cycle mutants are unable to fix N_2 in symbiosis with pea (*Pisum sativum*) and alfalfa (*Medicago sativa*), respectively (10-13). However, the TCA-cycle provides both reductant and biosynthetic precursors, so the abolition of N_2 fixation in these mutants could be due to insufficient NAD(P)H to directly power nitrogenase or, equally, result from biosynthetic deficiencies. In contrast, in soybean (*Glycine max*) bacteroids, the TCA-cycle is either dispensable for N_2 fixation or can be bypassed, with isocitrate dehydrogenase and 2-oxoglutarate dehydrogenase mutants of *Bradyrhizobium japonicum* able to fix N_2 at wild-type rates (14, 15). Moreover, standard midpoint potentials indicate that NAD(P)H is unlikely to donate electrons directly to ferredoxin [$E^{0\prime}$ for NAD^+/NADH is -320 mV, $NADP^+$/NADPH is -324 mV and ferredoxin (Fe^{3+}/Fe^{2+}) is -484 mV] (16, 17). Thus some other, as yet undefined mechanism, must exist to transfer electrons to nitrogenase in root nodule bacteroids.

Finally, N_2-fixing bacteroids in nodules formed by soybean and common bean (*Phaseolus vulgaris*) accumulate large quantities of the lipid-like polymer poly-β-hydroxybutyrate (PHB), while bacteroids from pea, alfalfa and clover (*Trifolium spp.*) apparently do not (18). While abolishing PHB synthesis does not adversely affect N_2 fixation rates in soybean and common bean (19-21), in *Azorhizobium caulinodans*, mutation of PHB synthase prevents N_2 fixation in both free-living and symbiotic forms (22), implying a fundamental role for PHB synthesis in at least some N_2-fixing rhizobia.

Determining how N_2 is fixed by bacteroids, arguably the second most important nutrient assimilation cycle after photosynthesis, requires an understanding of bacteroid carbon metabolism. Metabolic profiling, flux analysis, as well as mutational and N_2 fixation studies were used to investigate carbon flow in bacteroids. Remarkably, this reveals that the TCA-cycle is not the only sink for plant-derived carbon in symbiotic N_2 fixation; rather, pea bacteroids divert appreciable quantities of acetyl-CoA into the production of lipid or PHB. N_2-fixing bacteroids are therefore inherently lipogenic and this is probably a metabolic requirement for N_2 fixation.

Materials and Methods

Bacterial strains and culture conditions. Bacterial strains and plasmids used in this study are detailed in Table 1. *Rhizobium leguminosarum* bv. viciae (Rlv3841) was grown at 28°C on tryptone yeast extract (TY) (23) or acid minimal salts medium (AMS)(24) with succinate (20 mM) and NH_4Cl (10 mM) as the sole carbon and nitrogen source, respectively. Where appropriate, antibiotics were used at the following concentrations (in μg ml^{-1}): streptomycin (500), neomycin (80), spectinomycin (50), gentamycin (20) and ampicillin (50).

Metabolic flux analysis. Rlv3841 cells grown in succinate/NH_4Cl AMS were harvested at mid-log phase (OD_{600} ≈ 0.5) and subcultured into fresh AMS media to a starting OD_{600} of 0.02, with 20 mM [$^{13}C_4$]succinate (20% fractional abundance). Cells were harvested at OD_{600} of 0.3 and centrifuged at 8,500 x g for 5 min. The resulting pellet was washed with fresh AMS, centrifuged and the resulting cell pellet was extracted in 80% (v/v) ethanol at 80°C for 5 min, prior to centrifugation at 12,000 x g for 5 min. The supernatant containing the soluble amino acids, organic acids and sugars was dried by vacuum centrifugation. The insoluble pellet was rapidly frozen in liquid N_2 and freeze-dried. Protein in the insoluble fraction was hydrolysed to its component amino acids by incubation with 6 M HCl for 24 h at 100°C.

GC-MS analysis of derivatised amino acids, organic acids and sugars was performed on an Agilent 7890A GC/5975C quadrupole MS system as described elsewhere (25). Amino acids and organic acids were analysed after derivatisation using *N*-*tert*-butyldimethylsilyl-*N*-methyltrifluoroacetamide (MTBSTFA) or *N*-methyl-*N*-(trimethylsilyl)-trifluroacetamide (MSTFA); sugars were treated with methoxyamine hydrochloride and then derivatised with MSTFA. Protein-derived and soluble amino acids were examined separately. Mass isotopomer abundances were quantified using Chemstation and corrected for the presence of naturally occurring heavy isotopes introduced during derivatisation. The chemical fragments used for metabolic flux analysis are detailed in Supplementary Table 1.

Metabolic modelling was performed with 13C-FLUX (version 20050329) using the iterative procedure described before (25, 26). A complete description of the model, which also defines the network carbon atom transitions, is provided in Supplementary Table 2 and net fluxes are provided in Supplementary Table 3. During initial parameter fitting, fluxes to biomass outputs were allowed to vary, and the mean values from ten best-fit estimates were then used to constrain the network output flux values in subsequent simulations. Malate and oxaloacetate were combined into a single metabolite pool, as were phosphoenolpyruvate and pyruvate, to improve determinability of fluxes between these intermediates. No adjustments were required to compensate for the contribution of preexisting unlabelled pools of metabolites. Molar fluxes are reported relative to a succinate uptake flux of 1.

Material for metabolite profiling. To prepare samples of free-living Rlv3841, six independent cultures of Rlv3841, derived from six isolated colonies of the strain, were grown in AMS on a gyratory shaker at 250 rpm to an OD_{600} of 0.4. Cell pellets were collected by centrifugation (5000 x g, 5 min), washed with isolation buffer (8 mM K_2HPO_4, 2 mM KH_2PO_4, 2 mM $MgCl_2$) and stored at -80°C for later use in metabolite profiling.

To prepare bacteroid and nodule cytosolic samples, seeds of *P. sativum* cv. Avola were surfaced sterilised with 70% (v/v) ethanol for 30 s, rinsed once in sterile water and then immersed in a 2% (w/v) NaOCl solution for 2 min, prior to rinsing 10 times in sterile water. Seeds were sown into 2 L beakers containing washed and autoclaved fine grade vermiculite. Six independent cultures of the test strains Rlv3841 or RU116, derived from six isolated colonies of each strain, were prepared. A one ml aliquot of each culture was inoculated into a minimum of six pots, at cell densities between 5-9 x 10^7 cells ml^{-1}. Seeds were initially sown in duplicate and thinned to one plant per pot after seven days. Plants were watered once with 250 ml nitrogen-free nutrient solution as previously described (24) and were incubated in an illuminated environment-controlled growth room at 22°C on a 16 h day, 8 h night cycle.

Plants were harvested at 28 days post-inoculation (dpi) for metabolomic profiling. Approximately 1.5 g of nodule tissue was excised from plants from each set of pots. Nodules were ground in isolation buffer (8 mM K_2HPO_4, 2 mM KH_2PO_4, 2 mM $MgCl_2$) and the homogenate was passed through muslin and centrifuged (250 x g for 5 min) to remove plant debris before a further round of centrifugation (5000 x g, 10 min) to pellet the bacteroids. The resulting supernatant, representing the nodule cytosol fraction, was freeze-dried and the pellet, representing the bacteroid fraction, was washed twice with isolation buffer, centrifuged (5000 x g, 10 min) and the pellets frozen at -80°C for later use in metabolite profiling.

Metabolite profiling platform. Metabolomic profiles of free-living, bacteroid and nodule cytosol were each performed using non-biased, global metabolome profiling technology based on GC/MS and UHLC/MS/MS^2 platforms (27, 28) developed by Metabolon (www.metabolon.com). Six replicate samples from each treatment (free-living, bacteroid and nodule cytosol) were extracted using the automated MicroLab STAR® system (Hamilton, www.hamiltoncompany.com). Recovery standards were added prior to the first step in the extraction process for quality control purposes. To monitor total process variability a series of technical replicates were taken from a pool made from small aliquots of all the experimental samples. These were spaced evenly among the randomly ordered experimental samples and all consistently detected metabolites were monitored for reproducibility. Sample preparation was conducted using methanol extraction to remove the protein fraction while allowing maximum recovery of small molecules. The resulting extract was divided into two fractions; one for analysis by LC and one for analysis by GC. Samples were placed briefly on a TurboVap® (Zymark) to remove the organic solvent. Each sample was frozen and dried under vacuum. Samples were then prepared for the appropriate instrument, either LC/MS or GC/MS.

The LC/MS portion of the platform was based on a Waters ACQUITY UHPLC and a Thermo-Finnigan LTQ mass spectrometer, which consisted of an electrospray ionization source and linear ion-trap mass analyser. The sample extract was split into two aliquots, dried, then reconstituted in acidic or basic LC-compatible solvents, each of which contained 11 or more injection standards at fixed concentrations. One aliquot was analysed using acidic positive ion optimized conditions and the other using basic negative ion optimized conditions in two independent injections using separate dedicated columns. Extracts reconstituted in acidic conditions were gradient-eluted using water and methanol both containing 0.1% (v/v) formic acid, while the basic extracts, which also used water/methanol, contained 6.5 mM NH_4HCO_3. The MS analysis alternated between MS and data-dependent MS/MS scans using dynamic exclusion.

The samples destined for GC/MS analysis were re-dried under vacuum desiccation for a minimum of 24 h prior to being derivatised under dried N_2 using bistrimethyl-silyl-triflouroacetamide (BSTFA). The GC column was 5% phenyl and the temperature ramp was 40°C to 300°C, over a 16 min period. Samples were analysed on a Thermo-Finnigan Trace DSQ fast-scanning single-quadrupole gas chromatograph mass spectrometer using electron impact ionization.

Compound identification, data handling and statistical analysis. For metabolite profiling, identification of known chemical entities was based on comparison to metabolomic library entries of purified standards as previously described (28, 29). Statistical analysis was performed using the software packages Array Studio (Omicsoft) and R (http://www.r-project.org/). Where a given metabolite was not detected in a particular sample, then the observed minimum detected value for that metabolite from the analysis was assigned, under the assumption that missing values were not random, but resulted from the compound being below the limit of detection. Data for free-living and bacteroid samples were then normalised to protein content, as determined by Bradford assay(30). For the comparison of the bacteroids to the nodule cytosol, normalisation was performed by extracting proportional amounts of bacteroid and cytosolic fractions of matched starting samples. That is, the total yield of bacteroid and cytosolic fractions for each sample was known, and a constant percentage of each fraction was analysed in order to compare relative amounts of metabolites in each fraction. The statistical model utilized the matched pair nature of the samples to account for absolute differences between the samples. Welch's two-sample *t*-test was used to identify metabolites that differed significantly between experimental groups ($P < 0.05$) and the false discovery rate (FDR) was also calculated(31) to account for the multiple comparisons that normally occur in metabolomic-based studies ($Q < 0.1$). Thus, metabolites were considered to be significantly different if they met the criteria $P < 0.05$ and $Q < 0.10$.

Assessment of N_2 fixation. Plants for assessment of N_2 fixation were grown as described above in "Material for metabolite profiling", with the following exceptions. For measurement of N_2 fixation by acetylene reduction assay, plants were grown in 1 L pots and harvested at the onset of flowering (21 dpi). Whole plants were removed from growth pots and transferred to 250 ml sealed bottles. When rates of acetylene reduction of detached nodules were measured, nodules were excised and immediately transferred into a 25 ml bottle and assayed. Rates of N_2 fixation were determined by the amount of acetylene reduced after 1 h in an atmosphere consisting of 95% air-5% acetylene, as previously described (32). Following the acetylene reduction assay, bacteroid protein was quantified by excising nodules from roots and grinding in 40 mM HEPES (pH 7.0). The homogenate was passed through muslin and the eluate centrifuged (250 x g for 5 min) to remove plant debris. The supernatant was then centrifuged (5000 x g, 10 min) to pellet the bacteroids. Bacteroids were lysed by two rounds of ribolysing on a Fast Prep Ribolyser FP120 (BIO101/Savant) at a setting of 6.5 for 30 s, with samples on ice for 5 min in between. The protein content in the resulting supernatant was determined by Bradford assay (30) using the Pierce Coomassie assay kit (Pierce, cat# 23200) with BSA as the protein standard.

For assessment of N_2 fixation by plant biomass accumulation, plants were grown in 2 L pots and were supplied with 200 ml of additional sterile water at 28 dpi. Plants were then harvested at 47 dpi by cutting shoots below the hypocotyl and drying at 60°C for 48 h prior to weighing.

Lipid analysis. Bacteroids for lipids analysis were collected from nodules harvested from plants grown as described in the material for metabolite profiling section and harvested at 28 dpi. Nodules were ground in 20 mM HEPES buffer (pH 7.0) and purified by Percoll gradient (33). Cells of free-living Rlv3841 were grown in AMS with succinate and NH_4Cl and harvested at OD_{600} 0.4-0.6 by centrifugation (5000 x g for 10 min). Resultant bacteroid and cell pellets were stored at -80°C for later use. Bacteroid and cell pellets were lysed by ribolyser as described above and centrifuged (10,000 x g for 10 min). The supernatant was then centrifuged (20,000 x g for 20 min), prior to further ultracentrifugation (60,000 x g for 60 min) to remove cell membranes. The supernatant was concentrated by vacuum centrifugation prior to lipid quantification using the triglyceride determination kit (Sigma, cat# TR0100). Protein determination was performed using the Bradford assay as described above.

Mutant construction and phenotyping. To construct the *phaC2* (pRL100105) mutant of Rlv3841, primers pr1645 and pr1646 (see Supplementary Table 1) were used to amplify a 2.8 Kb of the region containing the gene and the PCR product was cloned into pJET1.2/blunt, giving plasmid pLMB834. The Ω-streptomycin/spectinomycin cassette from pHP45-ΩSmSp was cloned into the unique *Eco*RI site of pLMB834, to produce pLMB835. The BglII fragment from pLMB835 was cloned into pJQ200SK to produce pLMB839. Plasmid pLMB839 was then conjugated into strain Rlv3841, using pRK2013 as a helper plasmid, to produce *phaC2* mutants as previously described(5) resulting in LMB814. The mutation was confirmed by PCR mapping using primer pairs pr1648-potfarforward and pr1657-potfarforward. Strain LMB816, the *phaC1* (RL2098) *phaC2* (pRL100105) double mutant, was made by using the general transducing phage RL38 to lyse strain RU137. The kanamycin-marked *phaC1*::Tn5 mutation was then back-transduced into LMB814 to generate LMB816, as previously described (34) and the mutation was confirmed by PCR mapping with pr1647-potfarforward, pr1648-potfarforward and pr1647-Tn*5*-1 primer pairs. Assessment of N_2 fixation of the resulting mutants was performed as described above. Transmission electron microscopy was performed on nodules harvested from plants at 28 dpi and the methods for nodule sectioning, staining and microscopy are as detailed previously (20).

Results

Metabolic flux analysis of free-living rhizobia. Dicarboxylates are provided to bacteroids by plants to support N_2 fixation (3, 4), so the pathways operating in free-living *Rhizobium leguminosarum* bv. viciae 3841 (Rlv3841) growing on [$^{13}C_4$] succinate were quantified. The major flux of succinate metabolism in Rlv3841 was via fumarate to malate (Figure 1) and subsequently from malate to pyruvate and oxaloacetate to phosphoenolpyruvate. These fluxes would support the major metabolic requirements of cells growing on a TCA-cycle intermediate for synthesis of acetyl-CoA to supply the TCA-cycle and phosphoenolpyruvate for biosynthesis of sugars. Large fluxes were also detected in gluconeogenesis converting phosphoenolpyruvate to triose phosphates, in the oxidative decarboxylation of pyruvate to acetyl-CoA and in the TCA-cycle from oxaloacetate to 2-oxoglutarate. Overall, these fluxes are consistent with respiration of an obligate aerobe growing on a TCA-cycle intermediate as the sole carbon source.

Currently, metabolic flux analysis cannot be conducted on notoriously fragile isolated pea bacteroids (35). Nitrogenase activity, as measured by acetylene reduction, in isolated pea nodules collapsed 90 minutes after excision to less than 2% of that in nodules on roots (0.25 ± 0.03 *vs* 18.3 ± 2.5 nmol acetylene reduced. mg nodule^{-1}. h^{-1}). This precludes labelling of nodule metabolites to isotopic steady state under physiologically relevant conditions in an isolated system. Moreover, the likely slow rate of protein turnover in non-dividing bacteroids compromises the use of the labelling patterns of protein-derived amino acids to reflect those of their metabolic precursors. We therefore used metabolite profiling to examine the differences in levels of metabolic intermediates between cultured cells and bacteroids.

Bacteroid Central Metabolism. The metabolic profiles of free-living and bacteroid forms of Rlv3841 were analysed using non-biased, untargeted metabolome analysis (27, 28). Metabolites most highly elevated in bacteroids relative to free-living Rlv3841 were homoserine and asparagine (increased 105- and 58-fold respectively; Figure 2). Both were also high in the nodule cytosolic fraction relative to bacteroids (33- and 11-fold increased, Supplementary Table 5), in accordance with previous observations (36, 37), and consistent with their known plant origin. Asparagine is made in the plant cytosol as the primary nitrogen export product from nodules (35). Furthermore, free asparagine is not made by Rlv3841*,* which from analysis of its genome uses the GatCAB pathway to insert asparagine into proteins by charging asparaginyl-tRNA with aspartate and then transamidating aspartate to asparagine (38). In addition, catabolism of asparagine and homoserine is not up-regulated in bacteroids (39), nor do catabolic mutants show reduced N_2 fixation rates (40, 41), consistent with minor roles in symbiosis.

Our fundamental question is whether the TCA-cycle is altered during symbiotic N_2 fixation. The dicarboxylates malate, fumarate and succinate are the carbon sources for bacteroids *in planta* and levels of all three were increased in bacteroids relative to free-living cells (Figure 2). Moreover, these metabolites were also much higher in the plant nodule cytosol fraction relative to bacteroids (malate 14-, fumarate 20-; succinate 2.5-fold, Supplementary Table 5), consistent with active plant dicarboxylate synthesis.

Metabolism of dicarboxylates by bacteroids is via malic enzyme and phosphoenolpyruvate carboxykinase to pyruvate and phosphoenolpyruvate, respectively, with pyruvate subsequently oxidatively decarboxylated to acetyl-CoA (5-7). The intermediates of sugar metabolism such as 3-phosphoglycerate, fructose-6-phosphate and glucose-6-phosphate and the pentose phosphate pathway (ribulose-5-phosphate and xylulose-5-phosphate) were greatly reduced (Figure 2), suggesting little sugar synthesis occurs in bacteroids. Remarkably, pyruvate (5.5-fold down), acetyl-CoA (50-fold down), free coenzyme A (33-fold) and citrate (4.5-fold down) were much lower in bacteroids (Figure 2). In sharp contrast, the transcription and enzymatic activity of citrate synthase (RL2234, *icdB*) was increased 3.2- and 12-fold, respectively and increases in the activity and transcription of other enzymes of the decarboxylating arm of the TCA-cycle have been noted (39, 42). While such increased enzyme biosynthesis might indicate increased flux into the TCA-cycle, it is equally consistent with lower feedback inhibition of the synthesis and activity of enzymes by key intermediates such as acetyl-CoA and citrate (43, 44).

Carbon in the TCA cycle could also be channelled to glutamate, which is synthesised from 2-oxoglutarate by glutamine synthetase/glutamate synthase (GS/GOGAT)(45). However, glutamate levels were 20-fold lower in bacteroids relative to free living cells (Figure 2), consistent with GS/GOGAT activity being both low and not essential in mature bacteroids (46). Metabolites derived from glutamate, including glutathione and N-acetylglutamate were also reduced while levels of many other amino acids were either only slightly altered or unchanged in bacteroids (Figure 2).

However, steady state metabolite levels do not represent flux. Low levels of pyruvate, acetyl-CoA, coenzyme A and citrate in bacteroids may indicate a low rate of synthesis but can equally result from rapid turnover. Furthermore, metabolites may dramatically change concentrations during isolation of bacteroids from nodules. We addressed this by comparing wild-type with mutant bacteroids defective in the TCA-cycle, which should lead to different metabolite profiles. If low acetyl-CoA in wild-type bacteroids relative to free-living cells results from increased flux through the TCA-cycle, then TCA-cycle mutants should have elevated acetyl-CoA.

Metabolite profile of a TCA cycle mutant. We previously isolated several Tn*5* insertions in Rlv3841 genes encoding TCA-cycle enzymes (12). Malate dehydrogenase, succinyl-CoA synthetase and the E1 and E2 components of the 2-oxoglutarate dehydrogenase complex are transcribed from the *mdh-sucCDAB* operon (47). Mutations in *sucA* (RU156, RU724 and RU733) or *sucB* (RU726), encoding the E1 and E2 components of the 2-oxoglutarate dehydrogenase complex, respectively abolished 2-oxoglutarate dehydrogenase activity (12), resulting in plants that failed to reduce acetylene (Fix$^-$). Therefore, blocking the TCA-cycle in Rlv3841 prevents N_2 fixation. However, strain RU116, mutated in *sucD* (encoding the β-subunit of succinyl-CoA synthetase), originally scored as Fix$^-$ based on yellowing of plants and small nodules but retaining low levels of succinyl-CoA synthetase activity (12), we now show is able to reduce acetylene at 35% of the wild-type rate (Figure 3). This mutation may affect the number of bacteroids in nodules, total nodule mass or reduce nitrogenase activity. However, acetylene reduction per unit bacteroid protein and shoot dry matter of plants grown in nitrogen-free conditions inoculated with the *sucD* mutant were 45%- and-51% of the wild-type values, respectively (Figure 3). Therefore, *sucD* bacteroids have lowered N_2 fixation, presumably due to attenuation, but not complete blockage, of the TCA-cycle.

Metabolite profiles of the *sucD* mutant and wild-type bacteroids (Figure 4) show that while succinate levels were similar in RU116 and wild-type bacteroids, fumarate and malate were considerably lower in the mutant bacteroids, indicating reduced flux of carbon. Our key question concerns the decarboxylating arm of the TCA-cycle. Predictably for a mutant strain blocked in the TCA-cycle at succinyl-CoA synthetase, citrate levels were 11-fold higher in *sucD* than wild-type and intermediates derived from 2-oxoglutarate, such as glutamate, glutathione and 2-hydroxyglutarate, were all increased markedly (Figure 4). Therefore, attenuation of succinyl-CoA synthetase activity caused an accumulation of metabolites prior to the decarboxylating arm of the TCA-cycle. Thus, the TCA-cycle operates in bacteroids and reducing its activity also reduced N_2-fixation. Crucially though, while the level of pyruvate was similar between the two bacteroid types, no acetyl-CoA and free Coenzyme A were detected in the *sucD* mutant. If the only major route for acetyl-CoA metabolism is the TCA-cycle, its levels should rise dramatically in strain RU116 (*sucD*). This suggests acetyl-CoA has other large sinks independent of the TCA-cycle. The presence of alternative sinks for acetyl-CoA would explain its very low level in bacteroids compared to free-living bacteria. It would also have profound implications for our understanding of *Rhizobium*-legume symbioses as it suggests a major re-routing of central metabolism during N_2 fixation in pea bacteroids.

Lipids are a sink for acetyl-CoA in bacteroids. Apart from its complete oxidation in the TCA-cycle, the other major metabolic fate of acetyl-CoA is in lipogenesis. Two possible products of lipogenesis are poly-β-hydroxybutyrate (PHB) and fatty acids. Considerable attention has focussed on PHB because it is abundant in soybean and common bean bacteroids, although it is thought to be absent from mature N_2-fixing bacteroids from indeterminate nodulating plants including pea, alfalfa and clover. In contrast, there has been relatively little quantification of bacteroid lipids, which we sought to address.

There was a range of chain lengths and degrees of unsaturation in the free-fatty acids in both bacteroids and free-living succinate-grown cells (Table 2). Levels of long chain free-fatty acids (C16-C20) were higher in bacteroids than in either free-living bacteria or nodule cytosolic fractions. There were also significantly higher levels of monoacylglycerols, with bacteroids containing highly elevated levels of 1-linoleoylglycerol (>57-fold), 1-palmitoylglycerol (16-fold), 2-linoleoylglycerol (> 13-fold) as well as 1-stearoylglycerol (3.9-fold) and 2-oleoylglycerol (5.8-fold). Moreover, the less efficient N_2-fixing *sucD* mutant strain showed significantly lower levels of these lipid species compared to wild-type Rlv3841 bacteroids. The presence of these molecules at high levels in wild-type Rlv3841 suggests bacteroids use fatty acids as a sink for acetyl-CoA.

It was not possible to detect diacyclglycerols or triacylglycerols in these samples as they fall outside the polarity range and upper size limit of the GC- and LC-MS techniques used. Therefore, membrane-free extracts were isolated by ultracentrifugation and their glycerolipid level quantified by enzyme assay. Glycerolipids were 22-fold higher in bacteroids than free-living cells (62 ± 2.66 ng/mg protein vs 2.8 ± 1.26 ng/mg protein, respectively). Bacteroids channel a large proportion of acetyl-CoA away from the TCA-cycle and into lipids, suggesting related storage mechanisms may be utilised under N_2-fixing conditions.

Pea bacteroids of Rlv3841 accumulate PHB. PHB accumulation occurs in undifferentiated rhizobia in infection threads of pea nodules but is thought to be absent in bacteroids (20). When *R. leguminosarum* strain A34 was mutated in *phaC*, encoding a type I PHB synthase, it lacked detectable PHB in both infection thread bacteria and in bacteroids. This is consistent with the paradigm that bacteroids from indeterminate nodules such as pea and alfalfa do not make PHB in bacteroids. However, the genome of *R. leguminosarum* strain Rlv3841 has two PHB synthases: a type I on the chromosome (*phaC1,* RL2094) and a *phaE* (pRL100104) *phaC2* (pRL100105) type II PHB synthase on the symbiotic plasmid pRL10. The putative operon containing *phaEphaC2* is preceded by a consensus *nifA* promoter and was induced 7 to 40-fold in bacteroids, while *phaC1* was not upregulated (39). As PHB is another lipogenic end-product of acetyl-CoA metabolism, we investigated the symbiotic roles of these two PHB synthases in Rlv3841.

Previous work demonstrated that *phaC1* was active in free-living Rlv3841 as mutation of this gene reduced PHB accumulation in the mutant RU137 by 93% relative to wild-type (12), although the symbiotic performance of this *phaC1* mutant was not determined. Therefore, we isolated a *phaC2* single mutant (LMB814) and a *phaC1 phaC2* double mutant (LMB816) in Rlv3841 and assessed their symbiotic phenotype, along with the original *phaC1* mutant. While rates of N_2 fixation in *phaC1, phaC2* single and *phaC1 phaC2* double mutants were not significantly different from wild-type Rlv3841 (Supplementary Figure 1), examination of nodule sections by TEM showed that PHB accumulation was altered. Pea nodules containing wild-type Rlv3841 exhibited large PHB droplets in bacteria in infection threads and smaller bodies in mature bacteroids (Figure 5). Previously when small PHB droplets were observed in bacteroids it was assumed they were synthesized by bacteria in infection threads.

However, while the *phaC1* mutant harboured small PHB droplets in bacteroids, they were absent in the undifferentiated bacteria in infection threads. Conversely, PHB was largely absent in *phaC2* mutant bacteroids, but was abundant in bacteria occupying infection threads. Finally, PHB was absent from both bacteroids and bacteria in infection threads in the *phaC1 phaC2* mutant. Therefore, Rlv3841 has two functional PHB synthases: one active in free-living and undifferentiated bacteria (type I, PhaC1) and the other in bacteroids (type II, PhaE PhaC2). Although most sequenced rhizobia carry a type I PHB synthase, analysis of genome sequences shows other rhizobia contain *phaEphaC2* genes, including strains forming symbiotic interactions not usually thought to make PHB, such as *R. leguminosarum* bv. viciae VF39 (pea) and *R. leguminosarum* bv. trifolii TA1 (clover) (Integrated Microbial Genomes: https://img.jgi.doe.gov/cgi-bin/w/main.cgi). It is therefore likely that these other type II-harbouring bacteroids also accumulate PHB, as has been demonstrated for Rlv3841.

Discussion

The metabolism of free-living Rlv3841 growing on succinate as the sole carbon source is dominated by flux through the TCA-cycle as well as anaplerotic and biosynthetic reactions. However, while the TCA-cycle is essential for fully effective N_2 fixation in pea bacteroids, the accumulation of lipid shows a significant alternative fate for acetyl-CoA. Importantly, this observation is supported by the work of Miller and Tremblay (48) who showed that *S. meliloti* bacteroids from alfalfa nodules contain 34% of the total neutral lipid fraction as di- and triglycerides, whereas these lipids were undetected in free-living *S. meliloti*. Moreover, the extraordinary deposition of PHB in bacteroids from common bean and soybean is an extreme example of carbon storage and redox balancing that has hitherto lacked a coherent explanation, particularly since preventing synthesis in these symbioses does not prevent N_2

fixation (19-21). Here we show that bacteroids of some strains of *R. leguminosarum,* such as Rlv3841, make PHB via a putative *nifA*-dependent type II PHB synthase. Therefore, the paradigm that mature bacteroids from indeterminate nodules (such as those formed on pea, alfalfa and clover) do not synthesize PHB is incorrect. Most importantly, Rlv3841 bacteroids accumulate both PHB and lipid showing that even with acetyl-CoA incorporated into lipids, yet more acetyl-CoA accumulates in PHB. Thus, entry of acetyl-CoA into the TCA-cycle must be limited and implies that symbiotic N_2 fixation should be thought of as a fundamentally lipogenic process.

The complete oxidation of a mole of acetyl-CoA in the TCA cycle yields four moles of reducing equivalents (i.e. NAD(P)H or $FADH_2$). In free-living rhizobia, this reductant can be channelled to the aerobic respiratory chain, driving oxidative phosphorylation, or used as reductant in biosynthesis to fuel cell growth and division. However, mature pea bacteroids are in a metabolically active but non-dividing state. In addition, N_2 fixation in legume root nodules occurs at microaerobic O_2 concentrations, estimated at 3 to 57 nM (49, 50). This low O_2 level is likely to restrict bacteroid respiration and hence TCA cycle activity, thereby forcing acetyl-CoA into lipids. While it is theoretically possible to have large rates of electron flux to a high-affinity terminal oxidase such as *cbb₃* in bacteroids if O_2-flux is also high, the large scale production of lipids and PHB suggests this route is restricted. Instead, by channelling acetyl-CoA into lipid and PHB synthesis, bacteroids could overcome this metabolic constraint by consuming both carbon and reductant as NAD(P)H. Lipogenesis is a classic response of all domains of life to an excess of carbon and reductant that cannot be reoxidised by respiration or fermentation. Thus, free-living bacteria synthesise lipid when growth is nutritionally unbalanced, such as in O_2- or N_2-limited conditions (51, 52). During free-living N_2 fixation, both *Azotobacter beijerinckii* and *A. caulinodans* accumulate PHB and in *A. caulinodans*, PHB synthesis is essential to both free-living and symbiotic N_2 fixation (22, 53). Thus, bacteroids may be lipogenic as a physiological response to the microaerobic environment inside legume root nodules.

Although aerobically-growing free-living rhizobia and bacteroids differ in O_2 supply and ability to divide, the other obvious metabolic difference is the supply of ATP and reductant for bacteroid nitrogenase. Bacteroids must supply reductant and ATP to nitrogenase, requiring 8 moles of electrons and 16 moles of ATP to reduce one mole of N_2 (Equation 1). Although the electron source for nitrogenase is well understood in the free-living N_2-fixing bacteria *Klebsiella pneumoniae,* where electrons are transferred by NifJ (pyruvate:flavin oxidoreductase) and NifF (flavodoxin) complex from pyruvate to nitrogenase (54, 55), it is unknown for rhizobia. In the classical model in rhizobia, all reductant generated by metabolism, primarily as NAD(P)H, can be allocated to all processes including N_2 reduction or biosynthesis with excess reductant and ATP consumed by lipogenesis (Figure 6). However, the standard redox potentials of NADH and ferredoxin ($E^{0'}$ for $NAD^+/NADH$ is -320 mV and ferredoxin Fe^{3+}/Fe^{2+} -is 484 mV (16, 17)), suggest it is unlikely that NADH donates electrons directly to ferredoxin and then to nitrogenase. An alternative would be that a specific molecule acts as the low potential electron donor to nitrogenase, such as pyruvate oxidation by the NifJ-NifF complex in *K. pneumoniae* (54, 55). This process consumes four pyruvate molecules and produces four acetyl-CoA to generate the eight electrons needed by nitrogenase. Since this complex is not present in rhizobia, an alternative pathway is required. One possibility is that the <u>E</u>lectron <u>T</u>ransferring <u>F</u>lavoprotein (ETF) complex, FixABCX, interacts with pyruvate dehydrogenase, as shown by genetic suppressor analysis in

A. caulinodans (56). ETF complexes use electron bifurcation in anaerobic bacteria (57, 58), which might enable FixABCX to generate low potential electrons for reduction of ferredoxin and then N_2 (Figure 6). While unproven, such a mechanism requires eight moles of pyruvate to reduce one mole of N_2 and would exacerbate the reductant problem because acetyl-CoA oxidised by the TCA cycle would generate excess NAD(P)H. In the absence of convincing experimental evidence for the electron donation pathway to nitrogenase, we cannot complete a formal electron and reductant balance. However, Figure 6 illustrates how dramatically redox balance in bacteroids can be altered by the need for low potential electrons for N_2 reduction.

While *A. caulinodans,* must synthesize PHB during N_2 fixation (22), synthesis can be blocked in bacteroids of peas, alfalfa, common bean and soybean (19-21, 59, 60). The ability to prevent PHB synthesis and still have a functioning bacteroid may be explained by multiple storage sinks for acetyl-CoA including PHB, free fatty acids, glycerolipids and membrane phospholipids, with PHB itself being less important in these symbioses. Overall, bacteroids are highly lipogenic, with multiple lipid sinks for excess reductant. This applies to both determinate and indeterminate nodules and is likely to be an essential part of the energisation of nitrogenase and associated redox balance in all N_2-fixing symbioses.

Acknowledgments

This work was supported by the Biotechnology and Biological Sciences Research Council [grant number BB/F013159/1]. We thank Drs Graham O'Hara and Garth Maker (Murdoch University, Australia) for valuable input in preparing this manuscript. The collaboration between Dr Jason Terpolilli and Professor Philip Poole is supported by Murdoch University through the Sir Walter Murdoch Adjunct Professor Scheme.

References

1. **Olivares J, Bedmar EJ, Sanjuan J.** 2013. Biological nitrogen fixation in the context of global change. Mol Plant-Microbe Interact **26:**486-494.
2. **Herridge DF, Peoples MB, Boddey RM.** 2008. Global inputs of biological nitrogen fixation in agricultural systems. Plant Soil **311:**1–18.
3. **Udvardi M, Poole PS.** 2013. Transport and metabolism in legume-rhizobia symbioses. Ann Rev Plant Biol **64:**781-805.
4. **Terpolilli JJ, Hood GA, Poole PS.** 2012. What determines the efficiency of N_2-fixing *Rhizobium*-legume symbioses? Adv Micro Phys **60:**325-389.
5. **Mulley G, Lopez-Gomez M, Zhang Y, Terpolilli J, Prell J, Finan T, Poole P.** 2010. Pyruvate is synthesized by two pathways in pea bacteroids with different efficiencies for nitrogen fixation. J Bacteriol **192:**4944-4953.
6. **Driscoll BT, Finan TM.** 1993. NAD^+-dependent malic enzyme of *Rhizobium meliloti* is required for symbiotic nitrogen fixation. Mol Microbiol **7:**865-873.
7. **Driscoll BT, Finan TM.** 1997. Properties of NAD^+- and $NADP^+$-dependent malic enzymes of *Rhizobium* (*Sinorhizobium*) *meliloti* and differential expression of their genes in nitrogen-fixing bacteroids. Microbiology **143:**489-498.

8. **Preisig O, Anthamatten D, Hennecke H.** 1993. Genes for a microaerobically induced oxidase complex in *Bradyrhizobium japonicum* are essential for a nitrogen-fixing endosymbiosis. Proc Natl Acad Sci USA **90:**3309-3313.

9. **Delgado MJ, Bedmar EJ, Downie JA.** 1998. Genes involved in the formation and assembly of rhizobial cytochromes and their role in symbiotic nitrogen fixation. Adv Micro Phys **40:**191-231.

10. **Mortimer MW, McDermott TR, York GM, Walker GC, Kahn ML.** 1999. Citrate synthase mutants of *Sinorhizobium meliloti* are ineffective and have altered cell surface polysaccharides. J Bacteriol **181:**7608-7613.

11. **Koziol U, Hannibal L, Rodriguez MC, Fabiano E, Kahn ML, Noya F.** 2009. Deletion of citrate synthase restores growth of *Sinorhizobium meliloti* 1021 aconitase mutants. J Bacteriol **191:**7581-7586.

12. **Walshaw DL, Wilkinson A, Mundy M, Smith M, Poole PS.** 1997. Regulation of the TCA cycle and the general amino acid permease by overflow metabolism in *Rhizobium leguminosarum*. Microbiology **143:**2209-2221.

13. **Pardo MA, Lagunez J, Miranda J, Martinez E.** 1994. Nodulating ability of *Rhizobium tropici* is conditioned by a plasmid-encoded citrate synthase. Mol Microbiol **11:**315-321.

14. **Green LS, Emerich DW.** 1997. The formation of nitrogen-fixing bacteroids is delayed but not abolished in soybean infected by an α-ketoglutarate dehydrogenase-deficient mutant of *Bradyrhizobium japonicum*. Plant Physiol **114:**1359-1368.

15. **Shah R, Emerich DW.** 2006. Isocitrate dehydrogenase of *Bradyrhizobium japonicum* is not required for symbiotic nitrogen fixation with soybean. J Bacteriol **188:**7600-7608.

16. **Carter KR, Rawlings J, Orme-Johnson WH, Becker RR, Evans HJ.** 1980. Purification and characterization of a ferredoxin from *Rhizobium japonicum* bacteroids. J Biol Chem **255:**4213-4223.

17. **Loach PA.** 2010. Oxidation-reduction potentials, absorbance bands and molar absorbance of compounds used in biochemical studies, p 557-578. *In* Lundblad RL, Macdonald F (ed), Handbook of Biochemistry and Molecular Biology. CRC Press, Boca Raton.

18. **Sprent JI.** 2009. Legume Nodulation: A Global Perspective. Wiley-Blackwell, Oxford.

19. **Cevallos MA, Encarnacion S, Leija A, Mora Y, Mora J.** 1996. Genetic and physiological characterization of a *Rhizobium etli* mutant strain unable to synthesize poly-beta-hydroxybutyrate. J Bacteriol **178:**1646-1654.

20. **Lodwig EM, Leonard M, Marroqui S, Wheeler TR, Findlay K, Downie JA, Poole PS.** 2005. Role of polyhydroxybutyrate and glycogen as carbon storage compounds in pea and bean bacteroids. Mol Plant-Microbe Interact **18:**67-74.

21. **Quelas JI, Mongiardini EJ, Perez-Gimenez J, Parisi G, Lodeiro AR.** 2013. Analysis of two polyhydroxyalkanoate synthases in *Bradyrhizobium japonicum* USDA 110. J Bacteriol **195:**3145-3155.

22. **Mandon K, Michel-Reydellet N, Encarnacion S, Kaminski PA, Leija A, Cevallos MA, Elmerich C, Mora J.** 1998. Poly-β-hydroxybutyrate turnover in *Azorhizobium caulinodans* is required for growth and affects *nifA* expression. J Bacteriol **180:**5070-5076.

23. **Beringer JE.** 1974. R factor transfer in *Rhizobium leguminosarum*. J Gen Microbiol **84:**188-198.

24. **Poole PS, Schofield NA, Reid CJ, Drew EM, Walshaw DL.** 1994. Identification of chromosomal genes located downstream of *dctD* that affect the requirement for calcium and the lipopolysaccharide layer of *Rhizobium leguminosarum*. Microbiology **140:**2797-2809.

25. **Masakapalli SK, Kruger NJ, Ratcliffe RG.** 2013. The metabolic flux phenotype of heterotrophic *Arabidopsis* cells reveals a complex response to changes in nitrogen supply. Plant J **74:**569-582.

26. **Kruger NJ, Masakapalli SK, Ratcliffe RGJ.** 2012. Strategies for investigating the plant metabolic network with steady-state metabolic flux analysis: lessons from an *Arabidopsis* cell culture and other systems. J Exp Bot **63**.

27. **Lawton KA, Berger A, Mitchell M, Milgram KE, Evans AM, Guo L, Hanson RW, Kalhan SC, Ryals JA, Milburn MV.** 2008. Analysis of the adult human plasma metabolome. Pharmacogenomics **9:**383-397.

28. **Evans AM, DeHaven CD, Barrett T, Mitchell M, Milgram E.** 2009. Integrated, nontargeted ultrahigh performance liquid chromatography/electrospray ionization tandem mass spectrometry platform for the identification and relative quantification of the small-molecule complement of biological systems. Anal Chem **81:**6656-6667.

29. **Yobi A, Wone BW, Xu W, Alexander DC, Guo L, Ryals JA, Oliver MJ, Cushman JC.** 2012. Comparative metabolic profiling between desiccation-sensitive and desiccation-tolerant species of *Selaginella* reveals insights into the resurrection trait. Plant J **72:**983-999.

30. **Bradford MM.** 1976. A rapid and sensitive method for the quantitation of microgram quantities of protein utilizing the principle of protein-dye binding. Anal Biochem **72:**248-254.

31. **Storey JD, Tibshirani R.** 2003. Statistical significance for genomewide studies. Proc Natl Acad Sci USA **100:**9440-9445.

32. **Yates RJ, Howieson JG, Hungria M, Bala A, O'Hara GW, Terpolilli JJ.** 2016. Authentication of rhizobia and assessment of the legume symbiosis in controlled plant growth systems, p 73-108. *In* Howieson JG, Dilworth MJ (ed), Working with rhizobia. Australian Centre for International Agricultural Research, Canberra.

33. **Allaway D, Lodwig EM, Crompton LA, Wood M, Parsons R, Wheeler TR, Poole PS.** 2000. Identification of alanine dehydrogenase and its role in mixed secretion of ammonium and alanine by pea bacteroids. Mol Microbiol **36:**508-515.

34. **Buchanan-Wollaston V.** 1979. Generalized transduction in *Rhizobium leguminosarum*. J Gen Microbiol **112**.

35. **Lodwig E, Poole P.** 2003. Metabolism of *Rhizobium* bacteroids. Crit Rev Plant Sci **22:**37-78.

36. **Joy KW, Prabha C.** 1986. The role of transamination in the synthesis of homoserine in peas. Plant Physiol **82:**99-102.

37. **Prell J, Bourdes A, Karunakaran R, Lopez-Gomez M, Poole P.** 2009. Pathway of γ-aminobutyrate metabolism in *Rhizobium leguminosarum* 3841 and its role in symbiosis. J Bacteriol **191:**2177-2186.

38. **Min B, Pelaschier JT, Graham DE, Tumbula-Hansen D, Soll D.** 2002. Transfer RNA-dependent amino acid biosynthesis: an essential route to asparagine formation. Proc Natl Acad Sci U S A **99:**2678-2683.

39. **Karunakaran R, Ramachandran VK, Seaman JC, East AK, Mouhsine B, Mauchline TH, Prell J, Skeffington A, Poole PS.** 2009. Transcriptomic analysis of *Rhizobium*

leguminosarum biovar viciae in symbiosis with host plants *Pisum sativum* and *Vicia cracca*. J Bacteriol **191:**4002-4014.

40. **Vanderlinde EM, Hynes MF, Yost CK.** 2014. Homoserine catabolism by *Rhizobium leguminosarum* bv. viciae 3841 requires a plasmid-borne gene cluster that also affects competitiveness for nodulation. Environ Microbiol **16:**205-217.

41. **Huerta-Zepeda A, Ortuno L, Du Pont G, Duran S, Lloret A, Merchant-Larios H, Calderon J.** 1997. Isolation and characterization of *Rhizobium etli* mutants altered in degradation of asparagine. J Bacteriol **179:**2068-2072.

42. **McKay IA, Dilworth MJ, Glenn AR.** 1989. Carbon catabolism in continuous cultures and bacteroids or *Rhizobium leguminosarum* MNF3841. Arch Microbiol **152:**606-610.

43. **Tabrett CA, Copeland L.** 2000. Biochemical controls of citrate synthase in chickpea bacteroids. Arch Microbiol **173:**42-48.

44. **Dunn MF.** 1998. Tricarboxylic acid cycle and anaplerotic enzymes in rhizobia. FEMS Microbiol Rev **22:**105-123.

45. **Patriarca EJ, Tate R, Iaccarino M.** 2002. Key role of bacterial NH_4^+ metabolism in *Rhizobium*-plant symbiosis. Microbiol Mol Biol Rev **66:**203-222.

46. **Mulley G, White JP, Karunakaran R, Prell J, Bourdes A, Bunnewell S, Hill L, Poole PS.** 2011. Mutation of GOGAT prevents pea bacteroid formation and N_2 fixation by globally downregulating transport of organic nitrogen sources. Mol Microbiol **80:**149-167.

47. **Poole P, Reid C, East AK, Allaway D, Day M, Leonard M.** 1999. Regulation of the *mdh-sucCDAB* operon in *Rhizobium leguminosarum*. FEMS Microbiol Lett **176:**247-255.

48. **Miller RW, Tremblay PA.** 1983. Cytoplasmic membrane of *Rhizobium meliloti* bacteroids. I. Alterations in lipid composition, physical properties, and respiratory proteins. Can J Biochem Cell Biol **61:**1334-1340.

49. **Kuzma MM, Hunt S, Layzell DB.** 1993. Role of oxygen in the limitation and inhibition of nitrogenase activity and respiration rate in individual soybean nodules. Plant Physiol **101:**161-169.

50. **Appleby CA.** 1984. Leghaemoglobin and *Rhizobium* respiration. Ann Rev Plant Physiol **35:**443-478.

51. **Rehm BH.** 2010. Bacterial polymers: biosynthesis, modifications and applications. Nat Rev Microbiol **8:**578-592.

52. **Waltermann M, Steinbuchel A.** 2005. Neutral lipid bodies in prokaryotes: recent insights into structure, formation, and relationship to eukaryotic lipid depots. J Bacteriol **187:**3607-3619.

53. **Senior PJ, Beech GA, Ritchie GA, Dawes EA.** 1972. The role of oxygen limitation in the formation of poly-β-hydroxybutyrate during batch and continuous culture of *Azotobacter beijerinckii*. Biochem J **128:**1193-1201.

54. **Shah VK, Stacey G, Brill WJ.** 1983. Electron transport to nitrogenase. Purification and characterization of pyruvate:flavodoxin oxidoreductase. The *nifJ* gene product. J Biol Chem **258:**12064-12068.

55. **Nieva-Gomez D, Roberts GP, Klevickis S, Brill WJ.** 1980. Electron transport to nitrogenase in *Klebsiella pneumoniae*. Proc Natl Acad Sci USA **77:**2555-2558.

56. **Scott JD, Ludwig RA.** 2004. *Azorhizobium caulinodans* electron-transferring flavoprotein N electrochemically couples pyruvate dehydrogenase complex activity to N_2 fixation. Microbiology **150:**117-126.

57. **Bertsch J, Parthasarathy A, Buckel W, Muller V.** 2013. An electron-bifurcating caffeyl-CoA reductase. J Biol Chem **16:**11304-11311.

58. **Hess V, Gonzalez JM, Parthasarathy A, Buckel W, Muller V.** 2013. Caffeate respiration in the acetogenic bacterium *Acetobacterium woodii*: a coenzyme A loop saves energy for caffeate activation. Appl Environ Microbiol **79:**1942-1947.

59. **Povolo S, Tombolini R, Morea A, Anderson AJ, Casella S, Nuti MP.** 1994. Isolation and characterization of mutants of *Rhizobium meliloti* unable to synthesize poly-β-hydroxybutyrate. Can J Microbiol **40:**823-829.

60. **Aneja P, Charles TC.** 1999. Poly-3-hydroxybutyrate degradation in *Rhizobium* (*Sinorhizobium*) *meliloti*: isolation and characterization of a gene encoding 3-hydroxybutyrate dehydrogenase. J Bacteriol **181:**849-857.

61. **Johnston AWB, Beringer JE.** 1975. Identification of the *Rhizobium* strains in pea root nodules using genetic markers. J Gen Microbiol **87:**343-350.

62. **Prentki P, Krisch HM.** 1984. In vitro insertional mutagenesis with a selectable DNA fragment. Gene **29:**303-313.

63. **Quandt J, Hynes MF.** 1993. Versatile suicide vectors which allow direct selection for gene replacement in Gram-negative bacteria. Gene **127:**15-21.

64. **Figurski DH, Helinski DR.** 1979. Replication of an origin-containing derivative of plasmid RK2 dependent on a plasmid function provided *in trans*. Proc Natl Acad Sci USA **76:**1648-1652.

65. **Karunakaran R, Haag AF, East AK, Ramachandran VK, Prell J, James EK, Scocchi M, Ferguson GP, Poole PS.** 2010. BacA is essential for bacteroid development in nodules of galegoid, but not phaseoloid, legumes. J Bacteriol **192:**2920-2928.

Table 1 – Strains, plasmids and primers used in this study.

Strain, Plasmid or Primer	**Genotype or Sequence**	**Reference**
Strains		
Rlv3841	St^r derivative of *R. leguminosarum* bv. *viciae* strain 300	(61)
RU137	Rlv3841 *phaC1*::Tn*5*; Nm^r	(12)
RU116	Rlv3841 *sucD*::Tn*5*; Nm^r	(12)
RU156	Rlv3841 *sucA*::Tn*5*; Nm^r	(12)
RU724	Rlv3841 *sucA*::Tn*5-lacZ* ; Nm^r	(12)
RU725	Rlv3841 *sucC*::Tn*5-lacZ* ; Nm^r	(12)
RU726	Rlv3841 *sucB*::Tn*5-lacZ*; Nm^r	(12)
RU733	Rlv3841 *sucA*::Tn*5-lacZ*; Nm^r	(12)
LMB814	Rlv3841 *phaC2*::Ω; St^r Sp^r	This work
LMB816	Rlv3841 *phaC1*::Tn5 *phaC2*::Ω; St^r Nm^r Sp^r	This work
DH5α	*Escherichia coli* strain used for cloning: F$^-$ *ϕ80lacZΔM15 Δ(lacZYA-argF) U169 recA1 endA1 hsdR17*(r_k^-, m_k^+) *phoA supE44 thi-1gyrA96 relA1*	Invitrogen
Plasmids		
pJET1.2/Blunt	PCR product cloning vector; Ap^r	Thermo-Fisher
pHP45-ΩSmSp	pHP derivative with ΩSmSp cassette, Sm^r Sp^r	(62)
pJQ200SK	pACYC derivative, P15A origin of replication insertional mutagenesis inactivation vector, Gm^r Suc^s	(63)
pRK2013	Helper plasmid used for mobilizing plasmids. ColE1 replicon with RK2 *tra* genes, Km^r	(64)
pLMB834	pr1645-1646 PCR product (2.8 kbp) from pRL100105 (*phaC2*) cloned into pJET1.2/Blunt, Ap^r	This work
pLMB835	pLMB834 with ΩSmSp cassette from pHP45-ΩSmSp cloned into unique EcoRI site, Ap^r Sm^r Sp^r	This work
pLMB838	pJQ200SK with BglII fragment from pLMB835 containing *phaC2*:: Ω cloned into BamH1 site, Sm^r Sp^r Gm^r Suc^s	This work
Primers		
pr1645	AACGCTACAGCGCAACGCTC	This work
pr1646	ACTTTCTTCGCTCCCGTCGG	This work
pr1647	ACCCCGAAGACGCTCGTCAT	This work
pr1648	ATGATCGTGACGGCATCGGC	This work
potfarforward	GACCTTTTGAATGACCTTTA	(65)
Tn5-1	ATAGCCTCTCCACCCAAGC	This work

Table 2 – Comparison of fatty acids and monoacylglycerols detected in metabolite profiles showing the fold change in metabolite abundance, in Rlv3841 bacteroids relative to Rlv3841 free-living, nodule cytosol and *sucD* bacteroid samples, respectively. Boxes highlighted in red were significantly higher (P < 0.05 and Q < 0.1) and those in green were significantly lower (P<0.05 and Q<0.1) in Rlv3841 bacteroids, with un-highlighted boxes showing no significant difference.

	Fold Change in Metabolite Abundance (Amount in Rlv3841 bacteroids relative to other sample)		
Lipid Species	**Rlv3841 Bacteroids *vs.* Rlv3841 Free-living**	**Rlv3841 Bacteroids *vs.* Nodule cytosol**	**Rlv3841 Bacteroids *vs.* *sucD* Bacteroids**
Free Fatty Acids			
cis-vaccenate (18:1n7)	**1.99**	**5.91**	**4.00**
palmitoleate (16:1n7)	**8.20**	**4.87**	**2.94**
linolenate [α or γ (18:3n3 or 6)]	**23.0**	**4.09**	1.32
linoleate (18:2n6)	**18.7**	**3.62**	**2.13**
eicosenoate (20:1n9 or 11)	**8.39**	**2.91**	**2.56**
10-heptadecenoate (17:1n7)	**8.22**	**2.54**	1.19
dihomo-linoleate (20:2n6)	**3.81**	**2.50**	1.28
stearate (18:0)	**2.16**	**1.90**	**2.44**
palmitate (16:0)	**3.72**	**1.88**	**2.94**
margarate (17:0)	**3.94**	1.15	**1.89**
pelargonate (9:0)	0.75	**0.48**	**2.17**
heptanoate (7:0)	**0.19**	**0.19**	**0.46**
caproate (6:0)	**19.7**	**0.16**	0.71
caprylate (8:0)	1.45	**0.16**	0.75
isovalerate	1.30	**0.05**	**0.36**
Glycerolipids			
1-linoleoylglycerol (18:2)	**57.2**	**8.04**	**9.09**
2-linoleoylglycerol (18:2)	**13.2**	**5.38**	**6.25**
2-oleoylglycerol (18:1)	**5.83**	**3.16**	**2.78**
1-stearoylglycerol (18:0)	**3.86**	**0.33**	**3.85**
1-palmitoylglycerol (16:0)	**15.6**	**0.27**	**4.35**

Figure 1 - Flux map of central carbon metabolism for free-living *R. leguminosarum* Rlv3841, grown on succinate and NH_4Cl. Net fluxes are expressed on a molar basis relative to succinate uptake. The thickness of each arrow is proportional to net flux with the exception that fluxes < 1% of succinate uptake are indicated by broken arrows. Biosynthetic outputs are shown in solid rectangular boxes and metabolites treated as a single pool in the model are shown in dashed grey boxes. Flux identifiers, defined in Supplementary Table 2, are shown in italics. The precise values for the deduced fluxes are presented in Supplementary Table 4. Standard abbreviations are used for amino acids and metabolic intermediates, and PPP represent the reversible non-oxidative steps of the pentose phosphate pathway.

Figure 2 - Metabolite profile of Rlv3841 bacteroids *vs*. Rlv3841 free-living cells showing fold change in metabolite abundance relative to Rlv3841 bacteroids. Bacteroids were isolated from nodules from pea plants 28 days post-inoculation (dpi). Cells were harvested from log phase cultures grown in AMS broth with 20 mM succinate and 10 mM NH_4Cl as the carbon and nitrogen sources, respectively. Bolded intermediates were detected by metabolite profiling, with a statistically significant fold difference ($P < 0.05$ by Welch's T-test and $Q < 0.1$ for the False Discovery Rate) denoted with a red (increase) or green (decrease) arrow. A > sign indicates the metabolite was undetectable in either the free-living or the bacteroid sample, so the difference reported is therefore a lower limit estimate of the fold change. Intact arrows indicate single step enzyme catalysed reactions. Broken arrows indicate where two or more enzyme-catalysed steps are involved in a series of reactions. Abbreviations: UD, undetectable; BT, bacteroid; FL, free-living; GABA, γ-amino butyric acid; GSH, glutathione (reduced); GSSG, glutathione (oxidised); 2OG, 2-oxoglutarate; OAA, oxaloacetate; PEP, phosphoenolpyruvate.

Figure 3 – Symbiotic phenotype of *sucD* mutant (RU116) compared to wild-type Rlv3841. N_2 fixation as measured by acetylene reduction on whole plants at 28 dpi expressed on (a) per plant basis (n=6 per treatment) and (b) per unit bacteroid protein basis (n=6), where the significance value **P* < 0.05 was determined by Welch's T-test. A photograph of pea plants (c) at 47 dpi with uninoculated water control (WC), Rlv3841 and *sucD* (RU116) treatments. Mean shoot dry weights (d) of 42 dpi peas (n = 12 per treatment), where treatments not sharing a letter differ significantly at *P* < 0.05 (ANOVA and Tukey's HSD). In all cases, error bars represent standard errors of the means.

Figure 4 - Metabolite profile of *sucD* (RU116) bacteroids *vs*. Rlv3841 bacteroids showing fold change in metabolite abundance relative to *sucD* bacteroids. Bacteroids were isolated from nodules from pea plants 28 dpi. Bolded intermediates were detected by metabolite profiling, with a statistically significant fold difference (*P* < 0.05 by Welch's T-test and *Q* < 0.1 for the False Discovery Rate) denoted with a red (increase) or green (decrease) arrow. Intact arrows indicate single step enzyme catalysed reactions. Broken arrows indicate where two or more enzyme-catalysed steps are involved in a series of reactions. *sucD* bacteroids are attenuated in TCA-cycle enzymes post 2-oxoglutarate (2-OG). Abbreviations: UD, undetectable; GABA, γ-amino butyric acid; GSH, glutathione (reduced); GSSG, glutathione (oxidised); OAA, oxaloacetate; PEP, phosphoenolpyruvate.

Figure 5 – Transmission electron micrographs of pea nodules at 28 dpi. Wild-type Rlv3841 (a) bacteroids and (b) in an infection thread, both showing PHB droplets. Mutant *phaC1* (RU137) (c) bacteroids showing PHB accumulation, which is absent from (d) infection threads. Mutant *phaC2* (LMB814) (e) bacteroids where PHB droplets are largely absent, but

abundant in (f) in infection threads. Double mutant *phaC1 phaC2* (LMB816) (g) bacteroids and (h) in infection threads with PHB absent from both. Scale bars are 2 µm in a, c, e and g and 1 µm in b, d, f and h. Red arrows point to PHB droplets which appear white.

Figure 6 – Two possible pathways of electron allocation in N_2-fixing bacteroids. (a) In the first scenario, NADH supplies electrons directly to nitrogenase as well as providing ATP from oxidative phosphorylation. A minimum of two moles of malate are required to be oxidised to acetyl CoA to yield sufficient ATP and electrons to reduce one mole of N_2. (b) In the second scenario, electrons are supplied to nitrogenase via a tight coupling with PDH and electron bifurcation through FixABCX, requiring eight moles of malate to reduce one mole of N_2. The 16 moles of electrons liberated from the oxidation of eight moles of pyruvate could undergo electron bifurcation at FixABCX, resulting in eight electrons reducing CoQ via the Fix complex, while eight electrons are channelled to nitrogenase and N_2 fixation. The 16 ATP for N_2 fixation could be supplied from oxidative phosphorylation, for example the 8 electrons from FixABCX (i.e. $CoQH_2$) plus reoxidation of 8 $FADH_2$ generated in the TCA cycle. However, in this scheme if all eight acetyl CoA are oxidised in the TCA cycle, then the large yield of reductant (24 NADH plus the eight NADH from oxidation of malate by malic enzyme) could result in over-reduction of the electron carrier pool, requiring bacteroids to consume reductant and acetyl CoA through lipogenesis. The two models are not mutually exclusive as in (a), free NADH might also interact with FixABCX enabling low potential electrons to be generated by bifurcation for reduction of ferredoxin. Note that a P:2e$^-$ ratio of 2.5 is assumed for NADH and 1.5 for electrons entering the ETC at the level of CoQ. For simplicity we have not distinguished between NAD$^+$ and NADP$^+$ in this model. Abbreviations: CoQ,

Coenzyme Q; ETC, electron transport chain; ME, malic enzyme; N2ase, nitrogenase; PDH, pyruvate dehydrogenase.

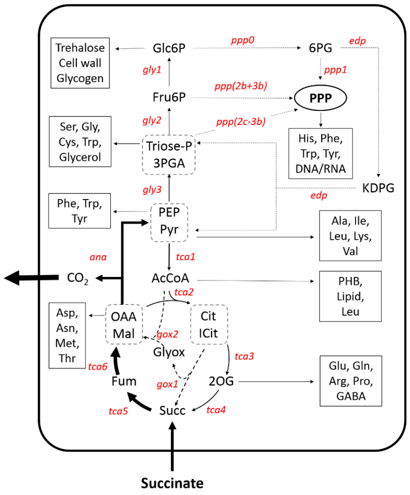
Trehalose
Cell wall
Glycogen
Glc6P
ppp0
6PG
edp
gly1
ppp1
Fru6P
ppp(2b+3b)
PPP
gly2
ppp(2c-3b)
Ser, Gly,
Cys, Trp,
Glycerol
Triose-P
3PGA
His, Phe,
Trp, Tyr,
DNA/RNA
KDPG
edp
gly3
Phe, Trp,
Tyr
PEP
Pyr
Ala, Ile,
Leu, Lys,
Val
ana
tca1
CO_2
AcCoA
PHB,
Lipid,
Leu
tca2
Asp,
Asn,
Met,
Thr
OAA
Mal
Cit
ICit
gox2
Glyox
tca3
tca6
Fum
gox1
2OG
Glu, Gln,
Arg, Pro,
GABA
tca5
Succ
tca4
Succinate

Figure 1.

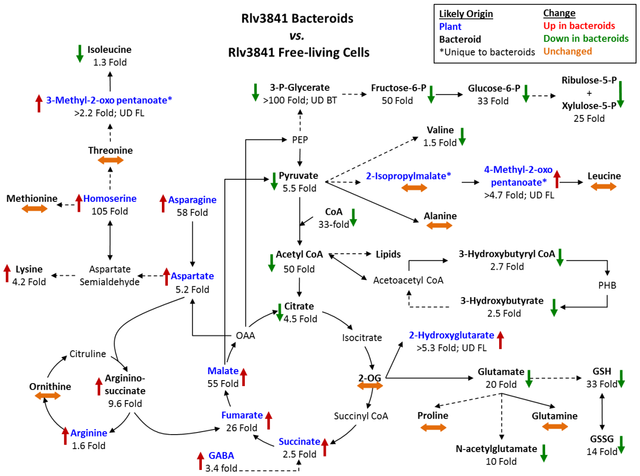
Rlv3841 Bacteroids
vs.
Rlv3841 Free-living Cells
Likely Origin
Plant
Bacteroid
*Unique to bacteroids
Change
Up in bacteroids
Down in bacteroids
Unchanged
Isoleucine
1.3 Fold
3-Methyl-2-oxo pentanoate*
>2.2 Fold; UD FL
Threonine
Methionine
Homoserine
105 Fold
Asparagine
58 Fold
Lysine
4.2 Fold
Aspartate
Semialdehyde
Aspartate
5.2 Fold
Citruline
Ornithine
Arginino-
succinate
9.6 Fold
Arginine
1.6 Fold
3-P-Glycerate
>100 Fold; UD BT
Fructose-6-P
50 Fold
Glucose-6-P
33 Fold
Ribulose-5-P
+
Xylulose-5-P
25 Fold
PEP
Valine
1.5 Fold
Pyruvate
5.5 Fold
2-Isopropylmalate*
4-Methyl-2-oxo
pentanoate*
>4.7 Fold; UD FL
Leucine
CoA
33-fold
Alanine
Acetyl CoA
50 Fold
Lipids
Acetoacetyl CoA
3-Hydroxybutyryl CoA
2.7 Fold
PHB
3-Hydroxybutyrate
2.5 Fold
Citrate
4.5 Fold
OAA
Isocitrate
2-Hydroxyglutarate
>5.3 Fold; UD FL
Malate
55 Fold
2-OG
Glutamate
20 Fold
GSH
33 Fold
Fumarate
26 Fold
Succinyl CoA
Proline
Glutamine
GSSG
14 Fold
Succinate
2.5 Fold
N-acetylglutamate
10 Fold
GABA
3.4 fold

Figure 2.

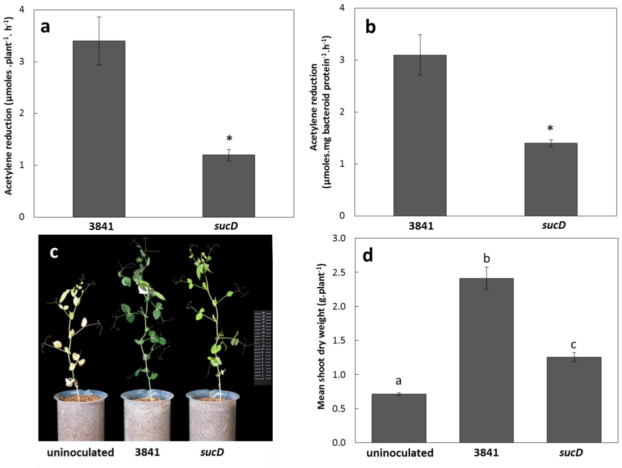
a
Acetylene reduction (µmoles .plant⁻¹. h⁻¹)
0
1
2
3
4
3841
sucD
*
b
Acetylene reduction (µmoles.mg bacteroid protein⁻¹.h⁻¹)
0
1
2
3
4
3841
sucD
*
c
uninoculated
3841
sucD
d
Mean shoot dry weight (g.plant⁻¹)
0.0
0.5
1.0
1.5
2.0
2.5
3.0
a
b
c
uninoculated
3841
sucD

Figure 3

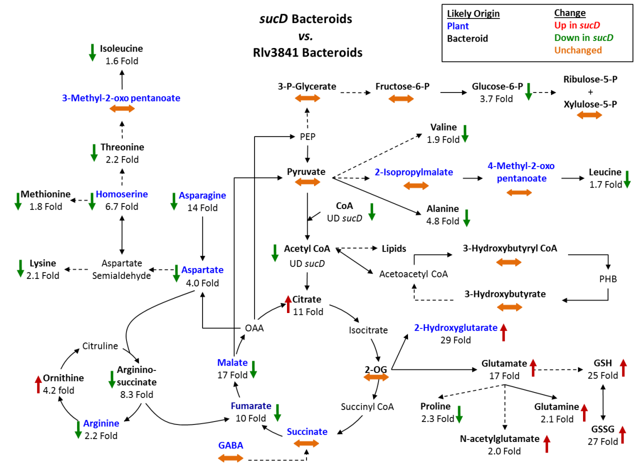
sucD Bacteroids
vs.
Rlv3841 Bacteroids
Likely Origin
Plant
Bacteroid
Change
Up in sucD
Down in sucD
Unchanged
Isoleucine
1.6 Fold
3-Methyl-2-oxo pentanoate
Threonine
2.2 Fold
Methionine
1.8 Fold
Homoserine
6.7 Fold
Asparagine
14 Fold
Lysine
2.1 Fold
Aspartate
Semialdehyde
Aspartate
4.0 Fold
3-P-Glycerate
Fructose-6-P
Glucose-6-P
3.7 Fold
Ribulose-5-P
+
Xylulose-5-P
Valine
1.9 Fold
PEP
Pyruvate
2-Isopropylmalate
4-Methyl-2-oxo
pentanoate
Leucine
1.7 Fold
CoA
UD sucD
Alanine
4.8 Fold
Acetyl CoA
UD sucD
Lipids
3-Hydroxybutyryl CoA
Acetoacetyl CoA
PHB
3-Hydroxybutyrate
Citrate
11 Fold
OAA
Isocitrate
2-Hydroxyglutarate
29 Fold
Citruline
Arginino-
succinate
8.3 Fold
Ornithine
4.2 fold
Arginine
2.2 Fold
Malate
17 Fold
Fumarate
10 Fold
Succinate
GABA
2-OG
Succinyl CoA
Glutamate
17 Fold
GSH
25 Fold
Proline
2.3 Fold
Glutamine
2.1 Fold
GSSG
27 Fold
N-acetylglutamate
2.0 Fold

Figure 4

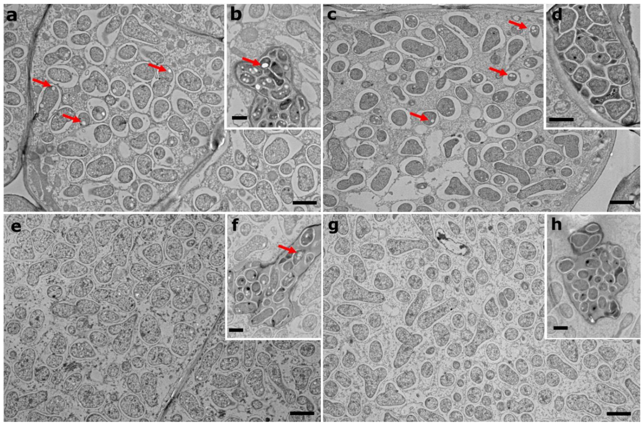

Figure 5

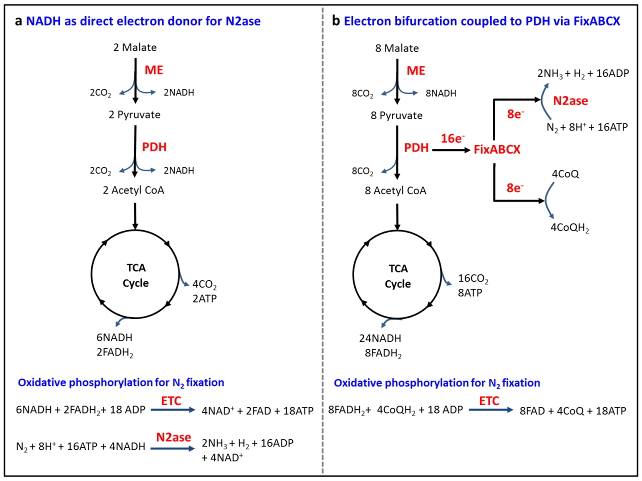
a NADH as direct electron donor for N2ase
2 Malate
ME
$2CO_2$
2NADH
2 Pyruvate
PDH
$2CO_2$
2NADH
2 Acetyl CoA
TCA Cycle
$4CO_2$
2ATP
6NADH
$2FADH_2$
Oxidative phosphorylation for N_2 fixation
$6NADH + 2FADH_2 + 18\ ADP \xrightarrow{ETC} 4NAD^+ + 2FAD + 18ATP$
$N_2 + 8H^+ + 16ATP + 4NADH \xrightarrow{N2ase} 2NH_3 + H_2 + 16ADP + 4NAD^+$
b Electron bifurcation coupled to PDH via FixABCX
8 Malate
ME
$8CO_2$
8NADH
8 Pyruvate
PDH
$16e^-$
FixABCX
$8e^-$
N2ase
$2NH_3 + H_2 + 16ADP$
$N_2 + 8H^+ + 16ATP$
$8e^-$
4CoQ
$4CoQH_2$
$8CO_2$
8 Acetyl CoA
TCA Cycle
$16CO_2$
8ATP
24NADH
$8FADH_2$
Oxidative phosphorylation for N_2 fixation
$8FADH_2 + 4CoQH_2 + 18\ ADP \xrightarrow{ETC} 8FAD + 4CoQ + 18ATP$

Figure 6